Soft Matter

Adaptable Eu-containing polymeric films with dynamic control of mechanical properties in response to moisture

Journal:	*Soft Matter*
Manuscript ID	SM-ART-12-2019-002440.R1
Article Type:	Paper
Date Submitted by the Author:	21-Jan-2020
Complete List of Authors:	Wei, Zichao; University of Connecticut, Department of Chemistry Thanneeru, Srinivas; University of Connecticut, Chemistry Rodriguez, Elena; University of Connecticut, Department of Chemistry Weng, Gengsheng; Ningbo University, He, Jie; University of Connecticut, Department of Chemistry

ARTICLE

Adaptable Eu-containing polymeric films with dynamic control of mechanical properties in response to moisture

Received 00th January 20xx,
Accepted 00th January 20xx

DOI: 10.1039/x0xx00000x

Zichao Wei,[a] Srinivas Thanneeru,[a] Elena Rodriguez,[a] Gengsheng Weng,[a,b,*] Jie He[a,c*]

ABSTRACT: Self-healing polymers often have a trade-off between healing efficiency and mechanical stiffness. Stiff polymers that sacrifice their chain mobility are slow to repair upon mechanical failure. We herein report adaptable polymer films with dynamically moisture-controlled mechanical and optical properties, therefore having tunable self-healing efficiency. The design of the polymer film is based on the coordination of europium (Eu) with dipicolylamine (DPA)-containing random copolymers of poly(*n*-butyl acrylate-*co*-2-hydroxy-3-dipicolylamino methacrylate) (P(*n*BA-*co*-GMADPA)). The Eu-DPA complexation results in the formation of mechanically robust polymer films. The coordination of Eu-DPA has proven to be moisture-switchable given the preferential coordination of lanthanide metals to O over N, using nuclear magnetic resonance and fluorescence spectroscopy. Water competing with DPA to bind Eu^{3+} ions can weaken the cross-linking networks formed by Eu-DPA coordination, leading to the increase of chain mobility. The *in-situ* dynamic mechanical analysis and *ex situ* rheological studies confirm that the viscofluid and the elastic solid states of Eu-polymers are switchable by moisture. Water speeds up the self-healing of the polymer film by roughly 100 times; while it can be removed after healing to recover the original mechanical stiffness of polymers.

Introduction

There has been an enormous amount of interest on synthetic polymers with reversible metal-ligand (M-L) binding, as inspired by mussel byssus threads that contain catechol moieties to coordinate mineral ions, *e.g.,* Fe^{3+}.[1-4] The M-L binding can break and reversibly reform under continuous equilibrium; therefore, synthetic polymers having M-L binding are self-healable upon mechanical failure.[5, 6, 3, 7] This is of particular importance towards improving the safety and lifetime of synthetic polymer materials. Compared to other non-covalent interactions,[8-11] the M-L binding is highly tuneable in terms of their binding strength and kinetics, known as the key parameters to tune self-healing efficiency.

Lanthanides are particularly useful in terms of their functionality and their large radius thus providing a high coordination number (*e.g.,* 9-12),[12-24, 7, 25] that can result in the high cross-linking density to improve the mechanical robustness of polymers.[13, 14, 16, 26] Meanwhile, the design of healable polymers has to balance the mechanical stiffness and self-healing efficiency. The materials with high mechanical strength and stiffness often sacrifice the chain mobility that imposes a large energy barrier to reform the polymer network.[27] This in turn slows down the chain diffusion and decreases the self-healing ability. In the current study, we propose the use of an old coordination trick, *i.e.,* the competitive binding of O and N to lanthanides,[28] as a means to balance the mechanical strength and self-healing efficiency. Using a tridentate ligand dipicolylamine (DPA) with three "N" atoms,[29, 30] we demonstrate that the coordination of europium (Eu) with DPA is moisture-switchable based on the coordination competition. Water competing with DPA to bind Eu^{3+} ions can dynamically tune the binding strength of Eu-DPA. The chain mobility of polymers as well as the self-healing efficiency, therefore, become controllable upon the use of water as a trigger (Figure 1a). When water binds to Eu^{3+} ions, the physical cross-linking density of the polymer decreases to allow for fast chain diffusion thus enabling extremely efficient healing. Once healed, moisture can be removed from the polymer film to recover its original mechanical strength. Compared to water-induced hydrogen bonding competition that also can drive efficient healing,[31-35] the mechanical strength of Eu-containing polymers is coupled with the emission property of Eu^{3+} ions.[36, 17, 37-39] Upon the coordination with water, the disruption of Eu-DPA coordination network not only weakens the mechanical strength of the polymer but also reduces the emission intensity of Eu^{3+} ions. The moisture-switchable M-L coordination, therefore, opens a new way to design the smart polymer materials potentially with an optical readout of their mechanical strength or states [40].

Results and discussion

The design of such Eu-containing polymers is shown in Figure 1a. The random copolymers of poly(*n*-butyl acrylate-*co*-2-hydroxy-3-dipicolylamino methacrylate) (denoted as P(*n*BA-*co*-GMADPA)) were prepared using reversible addition–fragmentation chain transfer polymerization.[41] The dipicoly-containing monomer, 2-hydroxy-3-dipicolylamino methacrylate (GMADPA), was synthesized using the ring opening reaction of glycidyl methacrylate with DPA (see SI for details and NMR).[42, 10] *n*BA was chosen as the co-monomer because of the low glass transition temperature (T_g) of P*n*BA (*ca.* -50 °C).[43] The synthetic details of GMADPA and polymers are given in experimental

[a] *Department of Chemistry, University of Connecticut, Storrs, Connecticut 06269, United States. Email: jie.he@uconn.edu (JH)*
[b] *School of Material Science and Chemical Engineering, Ningbo Key Laboratory of Specialty Polymers, Ningbo University, Ningbo 315211, China. Email: wenggengsheng@nbu.edu.cn (GW)*
[c] *Polymer Program, Institute of Materials Science, University of Connecticut, Storrs, Connecticut 06269, United States.*
†Electronic Supplementary Information (ESI) available: Characterization details of polymers, mechanical and healing measurements and supporting videos. See DOI: 10.1039/x0xx00000x

part. By varying the ratio of *n*BA and GMADPA, two random copolymers of P(*n*BA-*co*-GMADPA) were prepared as P(nBA$_{176}$-*co*-GMADPA$_{32}$) (P1) and P(nBA$_{210}$-*co*-GMADPA$_7$) (P2) (Table 1 and Figure S1). The NMR spectra of DPA, GMADPA and the two copolymers are shown in Figures S2-S3. The molecular weights of the two copolymers were calculated to be 33.7 and 29.3 kg·mol^{-1} based on the conversion of *n*BA measured from ^{1}H NMR. The GMADPA ligand ratio is around 15 mol% in P1 and 3 mol% in P2. P1 and P2 have a low T_g of -32.2 °C and -48.5 °C (Table 1 and Figure S4), respectively. Both polymers are viscous, brown liquids at room temperature (Figure 1b).

Table 1. Characterization of the two copolymers

No.	Polymers	Ligand Mole Fraction from NMR (%)	M_n (NMR) (kg.mol^{-1})	T_g (°C)
P1	P(nBA$_{176}$-*co*-GMADPA$_{32}$)	15	33.7	-32.2
P2	P(nBA$_{210}$-*co*-GMADPA$_7$)	3	29.3	-48.5

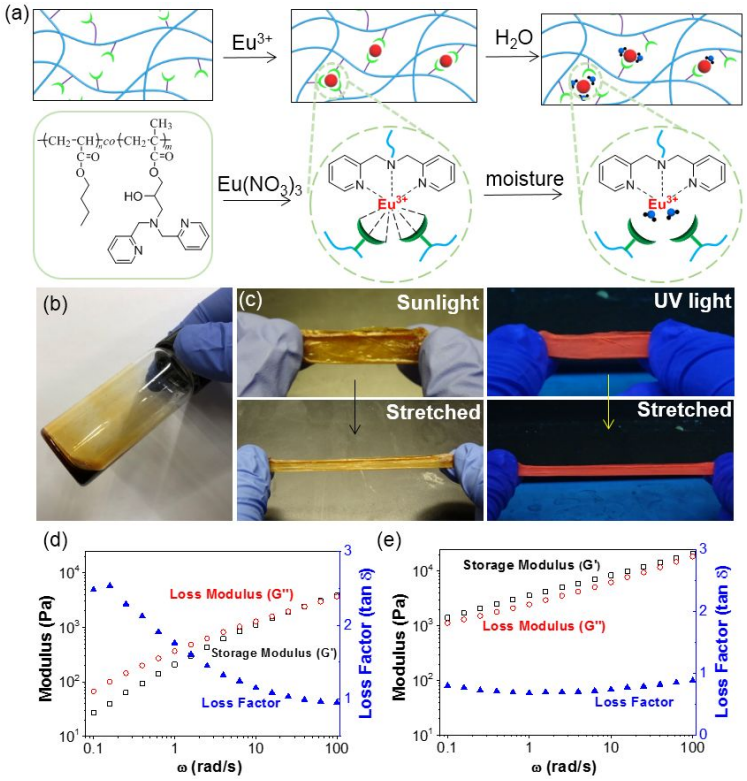

Figure 1. (a) Scheme of moisture-controlled Eu-DPA coordination in P(*n*BA-co-GMADPA). (b,c) Pictures showing the viscofluid state of P1 and the elastic solid state of the self-standing film of P1-Eu. In c, pictures were taken under sunlight (left) or under UV light (254 nm, right). (d,e) Rheological frequency sweep (0.1 to 100 rad/s) with a constant strain (1%) of P1 (d) and P1-Eu (e). G′ (open square), G′′ (open circle) and tan δ (filled triangle). The Eu-to-DPA ratio is 1:7 in (c-e).

To confirm Eu-DPA coordination in bulk and identify its effect on the mechanical properties of copolymers, the elastic behaviour of P1 with and without $Eu(NO_3)_3$ was compared using rheology. The frequency scan of the pure copolymer P1 shows a typical viscofluid where its loss modulus (G′′) is higher than the storage modulus (G′) across the frequency range of 0.1 to 100 rad/s (Figure 1c). This is confirmed by tan δ > 1 in the same range. Due to its low T_g, the pure P1 is a viscous liquid at room temperature (Figure 1b). On the contrary, the copolymer even with a low Eu-to-DPA ratio of 1:7 formed a self-standing film. The film was stretchable and red-emissive under UV light. The Eu-DPA coordination obviously impacts the mechanical properties of the copolymer. The moduli of the film showed a 10-time increase compared to that of the pure P1 (Figure 1e). The G′ of the Eu-containing film became higher than the G′′ indicating the formation of the physical networks via Eu-DPA coordination. When further increasing the content of Eu in P1, the increase in both moduli was seen in the elastic solid state (Figure S5). The moduli of the copolymer P1 with an Eu-to-DPA ratio of 1:3 are 2-order of magnitude higher than those of the pure copolymer (Figure S6). These results imply that the addition of Eu^{3+} ions can lead to the formation of elastic films. Similarly, the incorporation of $Eu(NO_3)_3$ with the copolymer P2 demonstrated the transition from a viscofluid to an elastic solid (Figure S7). However, the low DPA ratio of P2 limits the cross-linking density. Only a sticky film with poor mechanical strength was formed even at an Eu-to-DPA ratio of 1:3.[44-46]

Proton nuclear magnetic resonance (^{1}H NMR) spectroscopy was used to confirm Eu-DPA binding. We used the monomer GMADPA as a model compound to titrate with $Eu(NO_3)_3$ in tetrahydrofuran (THF). The four protons of pyridyl rings, labelled as *a*, *c*, *d* and *b* in Figure 2b and c, are well-resolved at 8.5, 7.6, 7.3 and 7.1 ppm, respectively. When titrated with $Eu(NO_3)_3$, the protons of pyridyl rings in GMADPA have pronounced resonance shifts and changes in peak intensities. In the presence of Eu^{3+}, the paramagnetic environment created by Eu^{3+} ions has largely changed the resonance feature of pyridyl rings.[47] This confirms the coordination of DPA with Eu^{3+} ions in solution. For P1 and P2, the four protons of pyridyl rings (Figures S8-S10) show a slight shift when bounded with $Eu(NO_3)_3$, compared to that of GMADPA; while, a 40% decrease of the peak intensity was seen. The

weaker paramagnetic effect in polymers is unclear but it is possibly a result of the presence of multi paramagnetic ions in polymers as reported previously.[48]

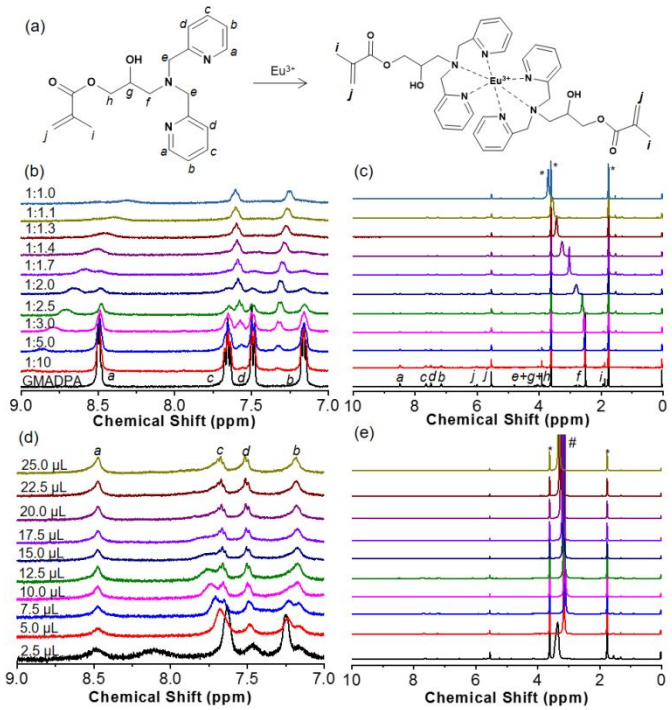

Figure 2. (a) Chemical structure of GMADPA. (b,c) ^{1}H NMR of GMADPA (black, bottom) and its titration spectra with $Eu(NO_3)_3$. (d,e) ^{1}H NMR reverse titration using water to an Eu-to-DPA ratio of 1:1 with a 2.5 µL incensement in 1 mL of d_8-THF. All spectra were measured in d_8-tetrahydrofunan (*). # is the peak for water.

GMADPA has an absorption peak around 260 nm (Figure S11), which can provide a weak "antenna effect" to enhance the emission of Eu^{3+} ions.[49, 50] The copolymer P1 containing Eu^{3+} ions had a strong red emission at 617 nm upon excitation at 272 nm (Figure 3a), corresponding to the $^5D_0 \rightarrow {}^7F_2$ transition of Eu^{3+} ions.[46] When titrating the copolymer P1 with $Eu(NO_3)_3$, the coordination number of Eu^{3+} ions can be analysed. The emission intensity at 617 nm is qualitatively plotted with Eu-to-DPA ratio as given in Figure 3b. The fluorescence intensity of Eu^{3+} ions showed a linear increase with the addition of Eu^{3+} before plateaued at an Eu-to-DPA ratio of 1:0.7, slightly lower than that of P2 (1:1) (Figure S12). This is likely due to the higher content of DPA in P1 that results in the in the loss of ligand accessibility, compared to P2.

Lanthanides preferentially coordinate to more electronegative elements, *e.g.,* O compared to N.[51-61] There are a number of examples that use Eu^{3+} complexes to pick up the trace amount of water from organic solvents as a means for water detection on the basis of the fluorescence quenching.[62, 63] One example from Mazzanti et al. show that water can even replace a strong tripod ligand, tris(2-pyridylmethyl)amine, from a few lanthanide metals including Eu.[28]

First of all, we confirmed that water is favourable to coordinate Eu^{3+} ions through the displacement of DPA ligands. This was carried out using the reverse titration of Eu-coordinated GMADPA with water, monitored by ^{1}H NMR (Figure 2d and e). The clear disruption of Eu-DPA was observed after immediately mixing with 2.5 µL of water (1 mL solution). The complete dissociation of Eu-DPA was seen with 15 µL of water. After the dissociation of Eu-DPA, the four protons of pyridyl rings recovered although they were slightly broadened (note that, Eu ions were not removed from the NMR solution). This suggests that water competes with DPA to disrupt Eu-DPA binding. The coordination competition is also characterized in Eu-coordinated P1. The recovery of the four pyridyl peaks was seen after the addition of water. The peak areas of *a* and *l* increased by ~20% with 10 µL of water, although further addition of water resulted in the precipitation of P1 (Figure S9).

When water binds to Eu^{3+} ions in the first coordination sphere, the O-H vibration as "oscillators" can quench the fluorescence of Eu^{3+} ions.[64, 65] Using fluorescence spectroscopy, we monitored the emission quenching of Eu^{3+} ions by water titrating (Figure 3). Only a small amount of water (*ca.* 1.5 vol%) can quench ~70% of the emission intensity of Eu^{3+} ions at 617 nm (see Figure S12 for P2). The fluorescence quenching also correlates with the number of water molecules per Eu^{3+} ion.[66, 63] We further used the lifetime study to confirm the presence of water in the first coordination sphere of Eu^{3+} ions (see Figure S13 for details). By increasing the amount of water in P2/THF solution up to 1.2 vol%, the lifetime of Eu^{3+} emission showed the linear dependence on the water concentration. This is indicative of the increase in number of the bound water on Eu^{3+} ions.

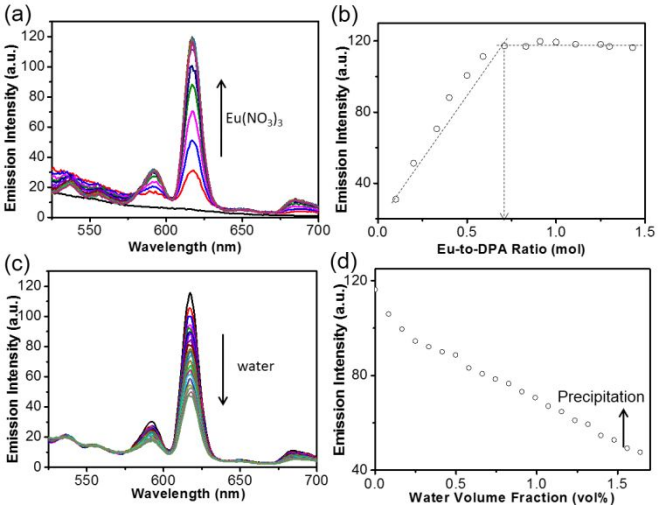

Figure 3. (a) Fluorescent spectra when titrating P1 in THF (1.67 mg/mL) using $Eu(NO_3)_3$. (b) Plotting emission intensity at 617 nm vs. Eu-to-DPA ratio. (c) Fluorescent spectra when reversely titrating Eu-containing P1 by adding water/THF (1/1, vol). The spectra were collected by stepwise adding 5 µL of water to the THF solution (3 mL) each time. (d) Emission intensity at 617 nm plotted against water concentration (vol%). The arrow indicates the polymer precipitation. All spectra were collected with an excitation wavelength of 272 nm.

We examined whether the Eu-DPA coordination could be disrupted in solid. Since P*n*BA is hydrophobic, the fluorescence quenching through water-competing coordination with DPA is expected to be slow due to the slow diffusion. To visualize the fluorescence change, a drop of Eu-P1 solution (50 µL) was cast on a glass slide and placed in a close chamber with a continuous flow of water-saturated N_2. The change in emission could be recorded using a digital camera (see Figure 4 and the supporting video). The red emission of the polymer film was substantially quenched when subjected to a 3-6 min flow of moisture-saturated N_2. *Ex situ* fluorescence measurements confirmed the decrease in the peak intensity at 617 nm with the continuous flow of moisture-saturated N_2. Qualitatively, 80% of the initial emission intensity was quenched after 15 min (Figure 4c). The fluorescence change of Eu^{3+} ions is reversible. The red emission of Eu^{3+} ions could be recovered after the

flow of dry N_2 for 5 min (Figure 4c). These findings show that the dynamic coordination of Eu-DPA is reversibly controllable through moisture. The coordination competition, therefore, brings the potential switching of cross-linking networks in polymers using water.

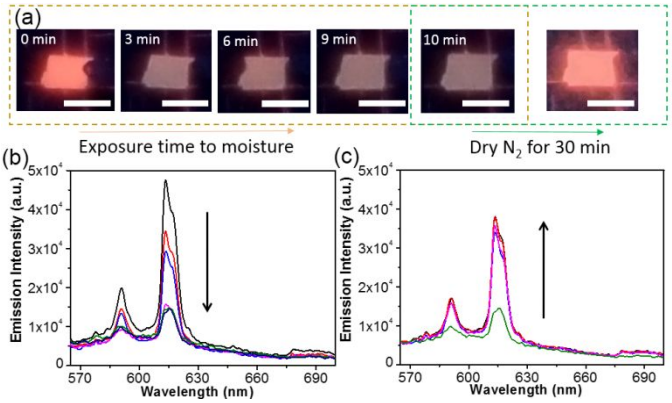

Figure 4. (a) Pictures recorded during fluorescence quenching and recovery. The P1 film with Eu-to-DPA ratio of 1:3 placed in a sealed chamber with the flow of moisture-saturated or dry N_2. Scale bars represent 0.5 cm. (b) The *ex situ* emission spectra of the P1 film containing Eu^{3+} ions under moisture-saturated N_2. The spectra were recorded every 3 min. (c) The emission spectra of the wetted film under dry N_2. The spectra were taken every 5 min. All spectra were collected using an excitation wavelength of 272 nm.

To estimate the impact of moisture on its mechenical strength and chain mobility, rheological behaviours of the P1 film containing Eu^{3+} ions (Eu-to-DPA = 1:3) were studied in the presence of water (Figure 5). Both moduli (G′ and G′′) displayed a continous decrease with a trace amount of water. The G′ at 100 rad/s decreased from 66 kPa to 10 kPa with 10 µL of water in ~15 mg of the P1 film. The two moduli almost overlopped across the range of scaning frequency (Figure 5C), suggesting that the films behaved like viscofluid in the presense of water. After drying by argon for 15 min, the magnitude of moduli recovered, and the elastic solid state was restored as well. Note that, the moduli were slightly higher for the recovered sample because the initial film was stored in air.

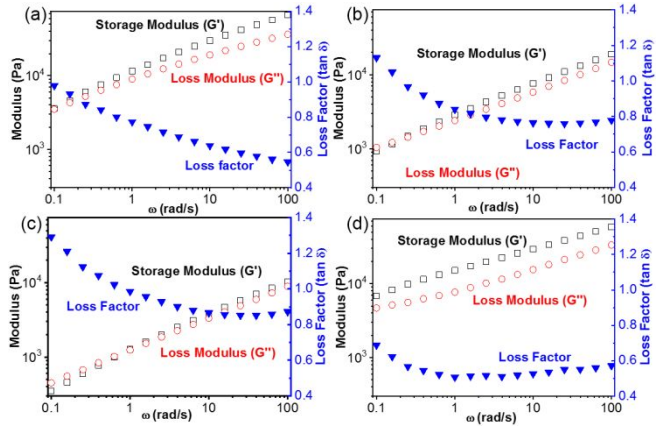

Figure 5. G′, G′′ and tan δ of the P1 film (~15 mg, Eu-to-DPA = 1:3) in response to water: (a) original; (b) 5 µL of water; (c) 10 µL of water; (d) dried with argon for 15 min. G′ (open square), G′′ (open circle) and tan δ (filled triangle).

The switching between the viscofluid and the elastic solid state is reversible. Using *in-situ* dynamic mechanical analysis (DMA), the moisture-switchable mechanical states are further revealed (Figure 6b). Before exposure to moisture, the initial G′ is greater than the G′′ in air, indicating the elastic solid state of the film. When the film was exposed to moisture, the values of G′ and G′′ gradually decreased. G′ dropped faster than G′′ and they became rather close to each other after 15 min (910 mechanical cycles). This suggests the disruption of the physical network of the polymer films since the coordination of Eu-DPA dissociated. When flowing with dry N_2, G′ and G′′ of the film quickly recovered. We carried out two hydration/dehydration cycles to confirm the reversibility of moisture-switching mechanical states.

The stress-strain curves of the copolymer P1 with different Eu-to-DPA ratios are shown in Figure 6a. The film with an Eu-to-DPA ratio of 1:7 was obviously more stretchable, as compared to the other two samples with higher ratios of Eu^{3+} ions. The maximum elongation at break reached 220±19% with a Young modulus of 1.0 MPa. As the content of Eu^{3+} ions increased, the stiffness of the films increased; and the maximum elongation at break decreased to 160±40% and 17±8% for the film with an Eu-to-DPA ratios of 1:5 and 1:3, respectively. Meanwhile, the Young modulus reached 39.5 MPa for the copolymer P1 with an Eu-to-DPA ratio of 1:3.

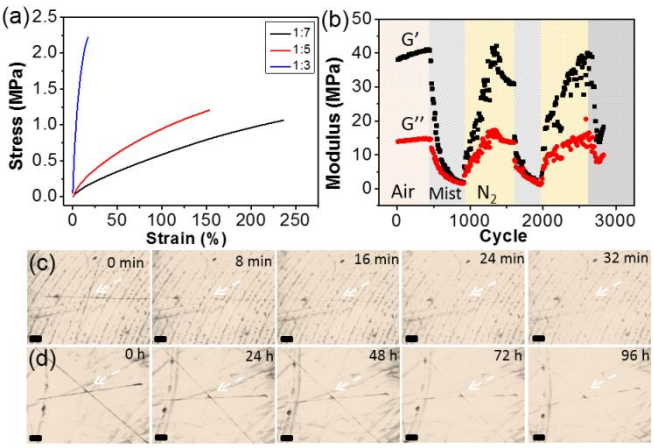

Figure 6. (a) Stress-strain curves of P1 with different Eu-to-DPA ratios (1:7, 1:5, 1:3). (b) Moisture-switchable mechanical states of P1-Eu from *in-situ* DMA measurement. DMA was proceeded using time sweep with a constant frequency of 1Hz and a constant strain of 2.5‰. Note that, the polymer film deformed in moisture/dry cycles, particularly upon exposure to a high humidity. Therefore, the moduli of the film in the final cycle did not overlap with those of the original film. (c,d) Self-healing of P1 with an Eu-to-DPA ratio of 1:3 in the presence of water (c) and in the absence of water (d). Scale bars are 200 µm. All measurements were carried out at room temperature.

Because the film becomes brittle at a high content of Eu^{3+} ions, a stronger physical network where the chain dynamics of polymers significantly slows down is expected. This in turn loses the dynamic properties endowed by strong M-L coordination. When such strong film fails mechanically or is wounded, the healing process is likely to be slow. As demonstrated in the Figure 6d, the cross wound on the surface of the P1 film with an Eu-to-DPA ratio of 1:3 took 96 h to heal at room temperature.

Since water competes with DPA to disrupt the M-L coordination, we can apply water locally on the wound, as to disrupt the coordination of Eu-DPA and accelerate the healing. After healing, the removal of water can recover the mechanical strength by reforming the coordination of Eu-DPA. This demonstration is given in Figure 6c.

The similar cross wound on the surface of the P1 film healed within 30 min in the presence of water, roughly 100-times faster compared to the healing at the absence of water.

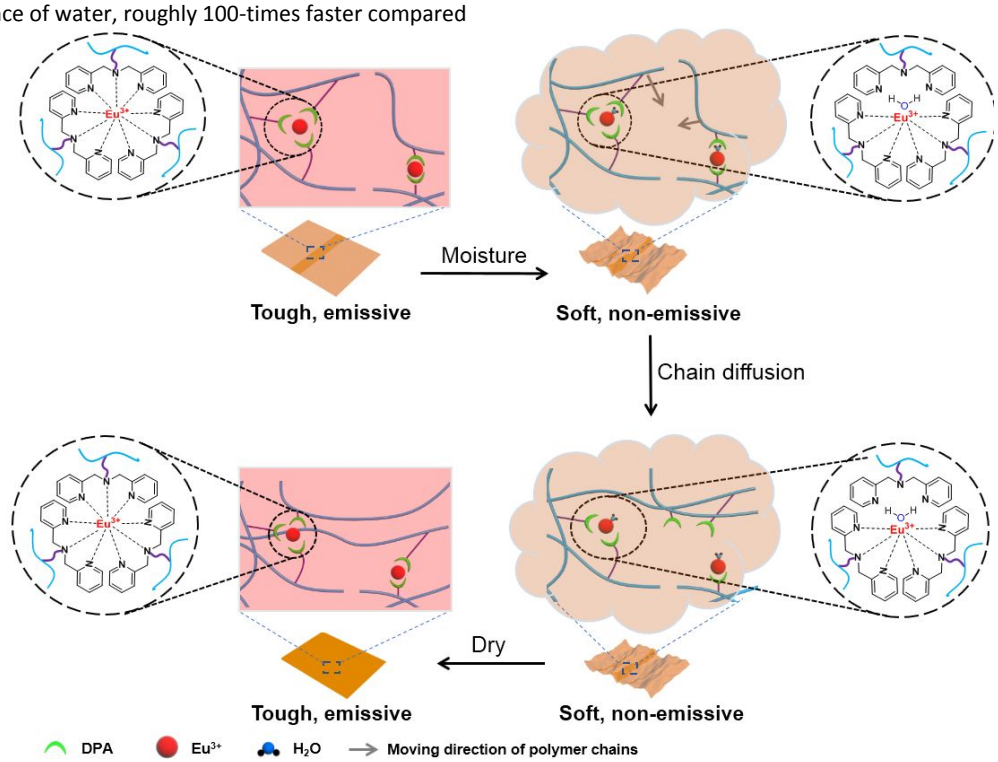

Scheme 1. Scheme of moisture-triggered self-healing mechanism of Eu-containing P(*n*BA-co-GMADPA).

To further confirm the recovery of mechanical strength after healing, the stress-strain curves are examined for the thin films healed at different healing times. To do so, two films of the copolymer P1 with an Eu-to-DPA ratio of 1:3 (length ~13.0 mm, width ~2.5 mm, thickness ~0.11 mm) were overlapped together with a cross-section length of ~2.5 mm.[67, 68] One set of samples were simply pressed together and left for 24, 48, and 72 h at room temperature before the mechanical test. The other set of samples were sprayed with water mist for 3 s and then pressed together for 15, 20, and 30 min. The films were dried under vacuum for another 30 min to remove water before mechanical test (Figure S14, Table S1). In the absence of water, the healed films showed a lower fracture stress after being stored for 24 h (0.49±0.43 MPa), 48 h (0.34±0.21 MPa) and 72 h (0.65±0.15 MPa) compared to the original film (2.21±0.64 MPa). All three samples fractured through sliding the two films at the healing regions (Figure S14d). Those results suggest that the two films did not completely diffuse across the interfaces even after 72 h; that is, the high cross-linking density results in low self-healing efficiency. On the contrary, the films healed in the presence of water had the comparable fracture stress after 15 min (1.7±0.17 MPa), 20 min (2.0±0.91 MPa) and 30 min (3.1±0.51 MPa). Moreover, the fracture occurred at the non-cut region after healing for 20 min (Figure S14c). This indicates that the overlapped interfaces healed and reinforced the stiffness of the interface of the two films.

Non-covalent M-L coordination has tuneable bonding strength when carefully choosing metals or ligands. It has been broadly used in self-healable polymeric materials,[69] due to reversible and dynamic nature of M-L coordination. Since lanthanide metals are much larger than base metals commonly used, the use of Eu^{3+} in coordination polymers enables a higher cross-linking density, as a physical network to strengthen the mechanical properties. As presented in our results (Figure 6a), the thin film of P1-Eu^{3+} is mechanically strong and highly emissive, given the sensitization of DPA to Eu^{3+} ions. The improved mechanical strength sacrifices the coordination dynamics and thus the polymer chain mobility.

Since water can replace DPA ligands to bind Eu^{3+} ions, the strong coordination networks of Eu-DPA can be weakened, leading to softening the film of P1-Eu^{3+}. When water as a competitive ligand to binds Eu^{3+} in the first coordination sphere,[70] this loosens Eu-DPA coordination (Scheme 2). The elastomers change from an elastic solid to a viscofluid state, since the copolymers have a low T_g. Those unbound or less bound polymer chains can diffuse across the wounded area to heal the film. When water binds to Eu^{3+} ions, the emission of Eu^{3+} ions is quenched and the film becomes non-emissive. After healing, water can be removed to restore the coordination network of Eu-DPA along with the mechanical strength and the emissive state of Eu^{3+} ions. Water therefore acts as a green "glue" to change the mechanical states/strength as demanded. To confirm the plasticizing effect plays a less important role in the chain dynamics of P*n*BA, the T_g of P1 and Eu^{3+}-containing P1 with different DPA-to-Eu ratios were measured with or without the presence of water (Figure S15 and Table S2). The T_g P1 is around -30 °C and it shows a minimum change in the presence of water, regardless of Eu^{3+} concentration. This suggests that water has a weak plasticizing effect to the hydrophobic P*n*BA, different from healable polymers with hydrogen bonds. In our case, water competes with DPA to bind Eu^{3+} and dynamically controls the physical cross-linking network. When the Eu-DPA coordination is weakened or disrupted, the self-healing occurs in the copolymers.

Conclusions

To summarize, we demonstrated moisture-adaptable polymer films with dynamically controlled mechanical and optical properties. The films were designed through Eu-DPA coordination in the random copolymers of P(*n*BA-co-GMADPA).

Using ^{1}H NMR and fluorescence spectroscopy, the coordination of Eu-DPA has proven to be moisture-switchable given the preferential coordination of lanthanide metals to O over N. With a low content of Eu^{3+} ions in the random copolymers, self-standing and mechanically robust films could be prepared. Since water binds to Eu^{3+} ions by competing DPA, the optical and mechanical states of the polymer films could be reversibly switched by water. The *in-situ* DMA measurements confirmed that the viscofluid and the elastic solid states of Eu-containing polymers were controllable by moisture. Moisture as a green "glue" was further used to efficiently speed up the self-healing process of the polymer film without altering its stiffness. We believe that the moisture-switchable M-L coordination provides a new way to remotely control the smart materials both mechanically and optically.

Experimental

Materials

*n*BA, GMA, 2,2-azobis(isobutyronitrile) (AIBN), 2-formylpyridine and the RAFT agent 4-cyano-2-(phenylcarbonothioylthio) pentanoic acid were purchased from Sigma-Aldrich. The *n*BA monomer was purified by passing an alumina column prior to use. AIBN was recrystallized from ethanol. $Eu(NO_3)_3{\cdot}6H_2O$ was purchased from Alfa-Aesar. 2-Aminomethylpyridine was purchased from Oakwood Chem. Sodium borohydride ($NaBH_4$) was from Tokyo Chemical Industry (TCI). Deionized water (High-Q Inc. 103Stills) with a resistivity of >10 MΩ was used throughout.

Synthesis of GMADPA

DPA was synthesized through the coupling reaction of 2-aminomethylpyridine with 2-formylpyridine.[71] 2-aminomethylpyridine (10 g, 92.6 mmol) was dissolved in 30 mL methanol in an ice/water bath. 2-formylpyridine (9.9 g, 92.6 mmol) was dissolved into 30 mL methanol and dropwise added into the methanol solution of 2-aminomethylpyridine. After 1 h, $NaBH_4$ (3.5 g, 92.6 mmol) slowly added to the mixture and stirring overnight. In order to purify DPA, the light-yellow solution mixture was firstly tuned to pH 3. The mixture was extracted with dichloromethane (DCM) for 3 times to remove unreacted reactants and the aqueous phase was collected. Excess Na_2CO_3 was then added to the aqueous solution to change the solution to pH 10. The solution was extracted with DCM at least 3 times and all oil phases were collected. The excess sodium sulfate was added to remove residual water in the oil phase. The DPA was obtained as a starting material to synthesize GMADPA after the removal of the solvents using a rotavap. ^{1}H NMR (in $CDCl_3$, Figure S2): δ (ppm) = 8.54 (d, 2H, py H^a), 7.61 (dt, 2H, py H^c), 7.34 (dd, 2H, py H^d), 7.12 (dt, 2H, py H^b), 3.95 (s, 4H, -CH_2-py).

DPA (4.09 g, 20.6 mmol) was mixed with GMA (2.92 g, 20.6 mmol) in 7 mL of N,N-Dimethylformamide (DMF). The mixture was heated to 100 °C for 5 h in a 25 mL round-bottom flask.[72] The reaction mixture was then poured into statured sodium bicarbonate solution. DCM was used to extract the product as GMADPA for 3 times and the crude product was obtained by concentrating the mixture with a rotavap. The crude product was washed with petroleum ether to remove the unreacted reactants. The final product was collected after the removal of the residual petroleum ether and dried under vacuum overnight. ^{1}H NMR (in $CDCl_3$, Figure S2): δ (ppm) = 8.55 (d, 2H, py H^a), 7.60 (dt, 2H, py H^c), 7.31 (dd, 2H, py H^d), 7.15 (dt, 2H, py H^b), 6.04 (s, 1H, CH_2=), 5.51 (s, 1H, CH_2=), 4.11 (q, 1H, -CH-O-), 3.97 (m, 2H, -O-CH_2-CH-), 3.89 (q, 4H, -CH_2-py), 2.75 (qd, 2H, -CH_2-N-), 1.89 (s, 3H, -CH_3). ^{13}C NMR (in $CDCl_3$, Figure S3): δ (ppm) 167.6, 159.2, 149.0, 136.9, 136.1, 125.6, 123.3,122.1, 67.2, 66.3, 60.1, 57.6, 18.2.

Synthesis of random copolymers, P(nBA-*co*-GMADPA)

P(*n*BA-*co*-GMADPA) was synthesized through reversible addition-fragmentation chain transfer polymerization. *n*BA (4.0 g, 31.2 mmol), GMADPA (1.5 g,4.5 mmol), AIBN (18.3 mg, 0.11 mmol) and 4-cyano-2-(phenylcarbonothioylthio) pentatonic acid (31.1 mg, 0.11 mmol), DMF (94.4 mg, 1.3 mmol) were dissolved into 2 mL of anisole in a 15 mL flask. The reaction mixture was degassed and purged with nitrogen (N_2) for 15 min. The flask was sealed then placed into oil bath preheated at 70 °C. The polymerization was carried out for 48 h. Then the copolymer was collected by diluted into DCM and precipitating in the mixture of methanol and water (1:1 vol) three times. From ^{1}H NMR spectrum (in $CDCl_3$), the number of repeat units of *n*BA and GMADPA was calculated to be 176 and 32, respectively, denoted as P($n\text{BA}_{176}$-*co*-GMADPA_{32}) (P1), based on the conversion of the two monomers. By varying the feed ratio between *n*BA and GMADPA, another polymer of P($n\text{BA}_{210}$-*co*-GMADPA_7) (P2) with a lower content of GMADPA was obtained. The molecular weight of the two polymers calculated to be 33.7 and 29.3 kg·mol^{-1}, respectively, based on the conversion of monomers. The summary of the two polymers is shown in Table 1.

Preparation of Eu-containing polymer films

Typically, the Eu-containing polymer film was prepared with different ratios of Eu-to-DPA. For example, 130 mg of the copolymer P1 was dissolved into 2 mL of THF. 20 mg of Eu $(NO_3)_3{\cdot}6H_2O$ solid dissolved into 300 μL THF to make the solution. 290 μL of the Eu solution was added into the polymer solution to make an Eu-to-DPA ratio of 3:1. In order to make uniform film, the mixture was sonicated for 5 min. The mixture was then casted on a Teflon mold (3.5 cm×3.5 cm) then all the solvent was first evaporated under room temperature. The film was then transferred into a vacuum oven and annealed at 80 °C for 6 h. The sample was cooled down overnight to obtain uniform films. The free-standing polymer film can be slowly peeled off from Teflon.

Characterization

^{1}H NMR measurements

^{1}H NMR measurements were carried out on a Bruker Avance 400 MHz NMR. In normal NMR measurements, the two polymer samples were dissolved in $CDCl_3$. For titration using $Eu(NO_3)_3{\cdot}6H_2O$ or water, 5 mg of P1 (as an example) was dissolved in 500 μL of d_8-THF (0.297 mM). At the same time, $Eu(NO_3)_3{\cdot}6H_2O$ was dissolved in d_8-THF (47.5 mM). 10 μL of $Eu(NO_3)_3$·solution was added to the above solution for each titration measurement. To study the binding competition with water, the titration was carried out by adding 5 μL of water/d_8-THF (1:1, vol) to the Eu-containing polymer solution in d_8-THF. The relative integral of peak *a* and peak *l* (Figure 2) was plotted against the ratio of Eu-to-DPA and water concentration.

Rheology measurements

The rheology of the copolymers with/without Eub was recorded on an AR-G2 (TA instrument) stress-controlled rheometer. The frequency sweep experiments were performed using a 20 mm aluminium parallel plate with a constant strain of 1%. The frequency ranges from 0.1 to 100 rad/s at 25 °C. Approximately 15 mg of polymers was used for each measurement. To study the binding competition with water, the rheological studies were conducted by

stepwise adding 5 µL of water. In order to measure the reversibility, the wetted polymer samples were dried by flowing argon for 15 min.

Fluorescence measurements

The optical images for self-healing experiments were recorded on an optical microscopy (AmScope ME 520TA). The P1 film with an Eu-to-DPA ratio of 1:3 was used. The film was scratched to make "cross" cuts using a clean razor. The sample was examined until the self-healing completed. In order to study the influence of the water on the self-healing efficiency, the water mist was sprayed on the surface of the scratched film for 3 s and the samples were examined under similar conditions. All optical images were recorded by 5× magnification.

The fluorescence spectroscopy was recorded on a Cary Eclipse fluorescence spectrophotometer. The emission of Eu^{3+} ions in the range of 500-700 nm was measured under excitation at 272 nm. The scan rate was 600 nm/min. To carry out the titration, 5 mg of P2 were dissolved into 3 mL of anhydrous THF. To this solution, 10 µL of the $Eu(NO_3)_3$·solution (12.3 mM) in anhydrous THF was added to the above polymer solution and the fluorescence spectrum was recorded. To measure the moisture-responsive emission of the Eu-containing polymers, the Eu-containing polymer solution was titrated with 5 µL of THF/water (1:1, vol). The measurements for the monomer and the copolymers were carried out using the same procedures. The lifetime was recorded and calculated using Cary Eclipse lifetime measurement. Typically, the copolymer P2 with an Eu-to-DPA ratio of 1:1 was dissolved in anhydrous THF. 5 µL of THF/water (1:1, vol) was continually added to the solution. The lifetime was recorded using the excitation at 272 nm and the emission at 617 nm.

Differential scanning calorimetry (DSC)

DSC was recorded using a TA Q20 calorimeter. For DSC measurements, the samples were equilibrated at -80 °C for 10 min then heated to 150 °C, followed by a cooling/hearting cycle at a rate of 5 °C/min.

DMA

The stress-strain tests were conducted on a TA Q800 instrument at room temperature in ramp mode and with a loading rate of 0.5 N/min. For *in-situ* measurement on the moduli against moisture exposure, the DMA time sweep measurements were used to characterize dynamic moduli change of the copolymer P1 with an Eu-to-DPA ratio of 1:3 under a constant frequency of 1 Hz with an amplitude of 10 µm (the length of the film is ~4.7 mm) at the room temperature. The changes in G' and G'' were observed in response to alternating switching water mist and the nitrogen flow. The healing films were prepared by cutting the films (thickness ~ 0.11 mm, length of 13.0 mm) into two pieces. The two halves were gently pressed together with cross section length of ~2.5 mm and then wait for a self-healing time of 24 h, 48 h and 72 h, respectively. The moisture driven healing films exposure at water mist for 3 seconds. Then two halves gently pressed together with cross section length of ~2.5 mm. Then the water stays on the film for 15 ,20 and 30 min. The films were dried in the vacuum for 30 min. The film was clamped with the clamp distance of ~7.5 mm. The Mechanical strain-stress curve recorded the fracture stress and elongation at break at room temperature.

Conflicts of interest

There are no conflicts to declare.

Acknowledgements

J.H. thanks financial support from the University of Connecticut, ACS petroleum research foundation and the National Science Foundation (CBET-1705566). G.W. is grateful for the financial support of Zhejiang Provincial Natural Science Foundation of China (grant No. LY19E030002), Ningbo Municipal Science and Technology Bureau (grant No. 2017A610051) and K. C. Wong Magna Fund in Ningbo University. This work was partially supported by the Green Emulsions, Micelles and Surfactants (GEMS) Center at the University of Connecticut.

Notes and references

1. N. Holten-Andersen, M. J. Harrington, H. Birkedal, B. P. Lee, P. B. Messersmith, K. Y. C. Lee and J. H. Waite, *PNAS*, 2011, **108**, 2651-2655.
2. M. Krogsgaard, M. A. Behrens, J. S. Pedersen and H. Birkedal, *Biomacromolecules*, 2013, **14**, 297-301.
3. L. Li, B. Yan, J. Yang, L. Chen and H. Zeng, *Adv. Mater.*, 2015, **27**, 1294-1299.
4. E. Filippidi, T. R. Cristiani, C. D. Eisenbach, J. H. Waite, J. N. Israelachvili, B. K. Ahn and M. T. Valentine, *Science*, 2017, **358**, 502-505.
5. S. Bode, L. Zedler, F. H. Schacher, B. Dietzek, M. Schmitt, J. Popp, M. D. Hager and U. S. Schubert, *Adv. Mater.*, 2013, **25**, 1634-1638.
6. D. Mozhdehi, S. Ayala, O. R. Cromwell and Z. Guan, *J. Am. Chem. Soc.*, 2014, **136**, 16128-16131.
7. Q. Zhang, S. Niu, L. Wang, J. Lopez, S. Chen, Y. Cai, R. Du, Y. Liu, J. C. Lai and L. Liu, *Adv. Mater.*, 2018, **30**, 1801435.
8. D. A. Davis, A. Hamilton, J. Yang, L. D. Cremar, D. Van Gough, S. L. Potisek, M. T. Ong, P. V. Braun, T. J. Martínez and S. R. White, *Nature*, 2009, **459**, 68.
9. S. Burattini, B. W. Greenland, D. H. Merino, W. Weng, J. Seppala, H. M. Colquhoun, W. Hayes, M. E. Mackay, I. W. Hamley and S. J. Rowan, *J. Am. Chem. Soc.*, 2010, **132**, 12051-12058.
10. G. R. Gossweiler, G. B. Hewage, G. Soriano, Q. Wang, G. W. Welshofer, X. Zhao and S. L. Craig, *ACS Macro Lett.*, 2014, **3**, 216-219.
11. W. Cui, J. Ji, Y.-F. Cai, H. Li and R. Ran, *J. Mater. Chem. A*, 2015, **3**, 17445-17458.
12. K. Mikami, M. Terada and H. Matsuzawa, *Angew. Chem. Int. Ed.*, 2002, **41**, 3554-3572.
13. J. B. Beck and S. J. Rowan, *J. Am. Chem. Soc.*, 2003, **125**, 13922-13923.
14. W. Weng, J. B. Beck, A. M. Jamieson and S. J. Rowan, *J. Am. Chem. Soc.*, 2006, **128**, 11663-11672.
15. E. G. Moore, A. P. Samuel and K. N. Raymond, *Acc. Chem. Res.* , 2009, **42**, 542-552.
16. J. R. Kumpfer, J. Jin and S. J. Rowan, *J. Mater. Chem.*, 2010, **20**, 145-151.
17. R. Shunmugam and G. N. Tew, *J. Am. Chem. Soc.*, 2005, **127**, 13567-13572.
18. R. Shunmugam and G. N. Tew, *J. Polym. Sci. A*, 2005, **43**, 5831-5843.
19. R. Shunmugam and G. N. Tew, *Polym. Adv. Technol.*, 2007, **18**, 940-945.
20. R. Shunmugam and G. N. Tew, *Macromol. Rapid Commun.*, 2008, **29**, 1355-1362.
21. R. Shunmugam and G. N. Tew, *Chem.: Eur. J*, 2008, **14**, 5409-5412.
22. R. Shunmugam and G. N. Tew, *Polym. Adv. Technol.*, 2008, **19**, 596-601.

23. R. Shunmugam, G. J. Gabriel, K. A. Aamer and G. N. Tew, *Macromol. Rapid Commun.*, 2010, **31**, 784-793.
24. P. Chen, Q. Li, S. Grindy and N. Holten-Andersen, *J. Am. Chem. Soc.*, 2015, **137**, 11590-11593.
25. N. Dey, D. Biswakarma and S. Bhattacharya, *ACS Sustainable Chemistry & Engineering*, 2018, **7**, 569-577.
26. J. Y. R. Silva, L. L. o. da Luz, F. G. M. Mauricio, I. B. Vasconcelos Alves, J. N. d. S. Ferro, E. Barreto, I. T. v. Weber, W. M. de Azevedo and S. A. Júnior, *ACS Appl. Mater. Interfaces*, 2017, **9**, 16458-16465.
27. Y. Yanagisawa, Y. Nan, K. Okuro and T. Aida, *Science*, 2018, **359**, 72-76.
28. L. Natrajan, J. Pécaut, M. Mazzanti and C. LeBrun, *Inorg. Chem*, 2005, **44**, 4756-4765.
29. S. Thanneeru, N. Milazzo, A. Lopes, Z. Wei, A. M. Angeles-Boza and J. He, *J. Am. Chem. Soc.*, 2019, **141**, 4252-4256.
30. S. Bhattacharya and S. S. Mandal, *Chem Comms*, 1996, **13**, 1515-1516.
31. K. Shanmuganathan, J. R. Capadona, S. J. Rowan and C. Weder, *Prog. Polym. Sci.*, 2010, **35**, 212-222.
32. A. E. Way, L. Hsu, K. Shanmuganathan, C. Weder and S. J. Rowan, *ACS Macro Lett.*, 2012, **1**, 1001-1006.
33. Z. C. Jiang, Y. Y. Xiao, Y. Kang, B. J. Li and S. Zhang, *Macromol. Rapid Commun.*, 2017, **38**, 1700149.
34. H. Cheng, Y. Huang, Q. Cheng, G. Shi, L. Jiang and L. Qu, *Adv. Funct. Mater.*, 2017, **27**, 1703096.
35. A. V. Salvekar, W. M. Huang, R. Xiao, Y. S. Wong, S. S. Venkatraman, K. H. Tay and Z. X. Shen, *Acc. Chem. Res*, 2017, **50**, 141-150.
36. Q. Ling, Q. Cai, E. Kang, K. Neoh, F. Zhu and W. Huang, *J. Mater. Chem.* , 2004, **14**, 2741-2748.
37. F. Rubio, F. García, H. Burrows, A. Pais, A. Valente, M. Tapia and J. García, *J. Polym. Sci. A*, 2007, **45**, 1788-1799.
38. B. M. McKenzie, R. J. Wojtecki, K. A. Burke, C. Zhang, A. Jákli, P. T. Mather and S. J. Rowan, *Chem. Mater.* , 2011, **23**, 3525-3533.
39. J. M. Stanley and B. J. Holliday, *Coord. Chem. Rev.*, 2012, **256**, 1520-1530.
40. X. Zhou, L. Wang, Z. Wei, G. Weng and J. He, *Adv. Funct. Mater.*, 2019, **29**, 1903543.
41. S. Thanneeru, W. Li and J. He, *Langmuir*, 2019, **35**, 2619-2629.
42. R. Gutierrez, E. Martín del Valle and M. Galan, *SEP PURIF REV.*, 2007, **36**, 71-111.
43. A. Buzin, M. Pyda, P. Costanzo, K. Matyjaszewski and B. Wunderlich, *Polymer*, 2002, **43**, 5563-5569.
44. D. E. Fullenkamp, L. He, D. G. Barrett, W. R. Burghardt and P. B. Messersmith, *Macromolecules*, 2013, **46**, 1167-1174.
45. K. Kawamoto, S. C. Grindy, J. Liu, N. Holten-Andersen and J. A. Johnson, *ACS Macro Lett.*, 2015, **4**, 458-461.
46. G. Weng, S. Thanneeru and J. He, *Adv. Mater.*, 2018, **30**, 1706526.
47. J. Hammell, L. Buttarazzi, C.-H. Huang and J. R. Morrow, *Inorg. Chem*, 2011, **50**, 4857-4867.
48. A. Meyers, A. Kimyonok and M. Weck, *Macromolecules*, 2005, **38**, 8671-8678.
49. E. R. Milaeva, D. B. Shpakovsky, Y. A. Gracheva, S. I. Orlova, V. V. Maduar, B. N. Tarasevich, N. N. Meleshonkova, L. G. Dubova and E. F. Shevtsova, *Dalton Trans.*, 2013, **42**, 6817-6828.
50. S. Achelle, J. Rodriguez-Lopez, F. Bureš and F. Robin-Le Guen, *Dyes Pigm.*, 2015, **121**, 305-311.
51. A. Trzesowska, R. Kruszynski and T. J. Bartczak, *Acta Crystallogr. B*, 2005, **61**, 429-434.
52. R. Díaz-Torres and S. Alvarez, *Dalton Trans.*, 2011, **40**, 10742-10750.
53. T. Mehdoui, J.-C. Berthet, P. Thuéry and M. Ephritikhine, *Dalton Trans.*, 2004, 579-590.
54. M. Brewer, D. Khasnis, M. Buretea, M. Berardini, T. Emge and J. Brennan, *Inorg. Chem*, 1994, **33**, 2743-2747.
55. P. Dorenbos, *Phys. Rev. B*, 2002, **65**, 235110.
56. A. de Bettencourt-Dias, S. Bauer, S. Viswanathan, B. C. Maull and A. M. Ako, *Dalton Trans.*, 2012, **41**, 11212-11218.
57. S. Mishra, S. Daniele, L. G. Hubert-Pfalzgraf and E. Jeanneau, *Eur. J. Inorg. Chem.*, 2007, **2007**, 2208-2215.
58. A. Beeby, R. S. Dickins, S. Faulkner, D. Parker and J. G. Williams, *ChemComm*, 1997, 1401-1402.
59. M. Heitzmann, F. Bravard, C. Gateau, N. Boubals, C. Berthon, J. Pécaut, M.-C. Charbonnel and P. Delangle, *Inorg. Chem*, 2008, **48**, 246-256.
60. M. Heitzmann, C. Gateau, L. Chareyre, M. Miguirditchian, M.-C. Charbonnel and P. Delangle, *New J. Chem.*, 2010, **34**, 108-116.
61. S. Wang, Y. Zhu, Y. Cui, L. Wang and Q. Luo, *Dalton Trans.*, 1994, 2523-2530.
62. A. K. Saha, K. Kross, E. D. Kloszewski, D. A. Upson, J. L. Toner, R. A. Snow, C. D. Black and V. C. Desai, *J. Am. Chem. Soc.*, 1993, **115**, 11032-11033.
63. M. Yao and W. Chen, *Anal. Chem.* , 2011, **83**, 1879-1882.
64. W. D. Horrocks Jr and D. R. Sudnick, *J. Am. Chem. Soc.*, 1979, **101**, 334-340.
65. A. Heller, *J. Am. Chem. Soc.*, 1966, **88**, 2058-2059.
66. S. Lis and G. R. Choppin, *Anal. Chem.* , 1991, **63**, 2542-2543.
67. Q. Wei, J. Wang, X. Shen, X. A. Zhang, J. Z. Sun, A. Qin and B. Z. Tang, *Sci. Rep.*, 2013, **3**, 1093.
68. N. Roy, E. Buhler and J. M. Lehn, *Polym. Int.*, 2014, **63**, 1400-1405.
69. D. W. Balkenende, S. Coulibaly, S. Balog, Y. C. Simon, G. L. Fiore and C. Weder, *J. Am. Chem. Soc.*, 2014, **136**, 10493-10498.
70. S. V. Eliseeva and J.-C. G. Bünzli, *Chem. Soc. Rev.*, 2010, **39**, 189-227.
71. J. N. Hamann, M. Rolff and F. Tuczek, *Dalton Trans.*, 2015, **44**, 3251-3258.
72. S. Thanneeru, S. S. Duay, L. Jin, Y. Fu, A. M. Angeles-Boza and J. He, *ACS Macro Lett.*, 2017, **6**, 652-656.

ARTICLE

Table of Contents

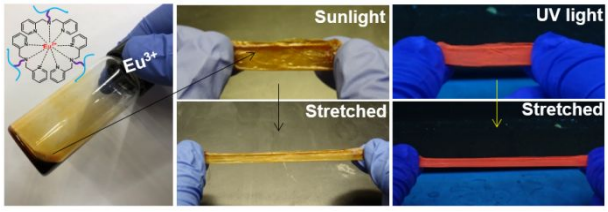

Moisture that competes with dipicolylamine to bind Eu dynamically controls the mechanical and optical properties of polymer films, as well as their self-healing efficiency.